Nanoscale

Accepted Manuscript

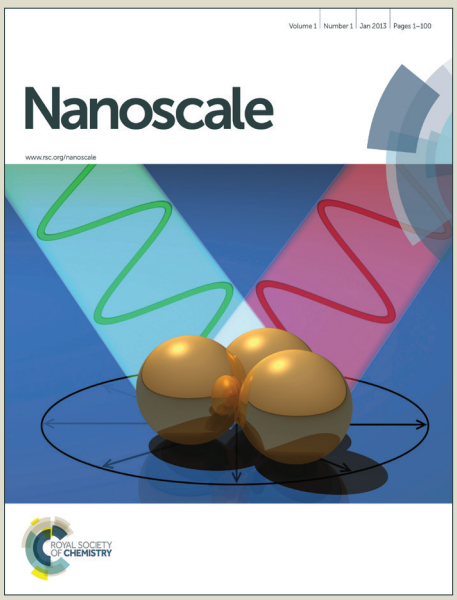

ROYAL SOCIETY OF CHEMISTRY

www.rsc.org/nanoscale

Cite this: DOI: 10.1039/c0xx00000x

www.rsc.org/xxxxxx

ARTICLE TYPE

Polypeptide cationic micelles mediated knockdown of ZEB1inhibits metastasis and sensitizes chemotherapeutic drug for cancer therapy

Shengtao Fang, Lei Wu, Mingxing Li, Huqiang Yi, Guanhui Gao, Zonghai Sheng, Ping Gong, Yifan Ma* and Lintao Cai*

Received (in XXX, XXX) Xth XXXXXXXXX 20XX, Accepted Xth XXXXXXXXX 20XX
DOI: 10.1039/b000000x

Metastasis and drug resistance are the main cause for the failure in clinical cancer therapy. Emerging evidence suggests an intricate role of epithelial–mesenchymal transition (EMT) and cancer stem cells (CSCs) in metastasis and drug resistance. The EMT-activator ZEB1 is crucial in malignant tumor progression by linking EMT-activation and stemness-maintenance. Here, we used multifunctional polypeptide micelle nanoparticles (NP) as nanocarriers for delivery of ZEB1 siRNA and doxorubicin (DOX). The nano-carriers could effectively delivere siRNA to the cytoplasm and knockdown the target gene in H460 cells and H460 xenograft tumor, leading to reduced EMT and repressed CSC properties *in vitro* and *in vivo*. The complex micelle nanoparticles with ZEB1 siRNA (siRNA-NP) significantly reduced the metastasis in lung. When DOX and siRNA were co-delivered by the nano-carriers (siRNA-DOX-NP), a synergistic therapeutic effect was observed, resulting in dramatically inhibition of tumor growth in H460 xenograft model. These results demonstrated that siRNA-NP or siRNA-DOX-NP complex targeting ZEB1 could be developed into a new therapeutic approach for non-small cell lung cancer (NSCLC) treatment.

Introduction

Metastasis and drug resistance are great challenge in the development of improved cancer therapies. Increasing evidence indicates that epithelial–mesenchymal transition (EMT) and cancer stem cells (CSCs) play critical role in metastasis and drug resistance.[1-6] EMT promotes Invasion and metastasis by triggering cellular mobility and dissemination. Cancer cells that have undergone an EMT can generate CSC-like phenotype,[7, 8] which contributes to drug resistance.[2, 9, 10] In addition, it is reported that chemotherapy drugs such as DOX can activate EMT and induce CSCs resulting in drug resistance.[11] The transcriptional repressor ZEB1, a key regulator of EMT, promotes metastasis and tumorigenicity not only by enhancing cell dissemination through EMT, but also by creating and maintaining a stem cell phenotype.[12, 13] Recent study have shown that ZEB1 could also enhance tumorigenicity by driving non-CSC to CSC conversion in basal breast cancer.[14] Moreover, ZEB1 is often aberrantly expressed in various carcinomas, knockdown ZEB1 expression through RNAi can dramatically inhibit the growth of lung cancer cells and malignant Pleural mesothelioma cells.[15-17] Thus, targeting ZEB1 could be a promising therapeutic strategy for improved cancer therapies.[13-15]

RNAi-based therapies have the ability to target oncogenes or pathways which are crucial to cancer progress and metastasis, opening the door for new strategies of cancer treatment. However, clinical use of siRNA in therapy is hindered by its short half-life in blood and poor bioavailability. Efficient and safe delivery systems are needed to realize its full therapeutic potential. The use of nanocarriers to deliver siRNA, prevents both renal clearance and RNase degradation, significantly prolongs half life in blood, showing great promise for cancer therapy.[18-21] Traditional chemotherapy drugs encapsulating in nanocarriers, increase the solubility of the drug, enhance intratumoral drug concentration，decrease the toxicity to healthy tissues,[22, 23] and are currently in the clinics.[24] More importantly，it has been reported that co-delivering traditional chemotherapy drugs and siRNA together in the same multifunctional delivery system is more effective for cancers treatments with synergistic or combined effects.[25-28] Polycations nanoparticles are the currently most widely used non-viral vectors for drugs and siRNA co-delivery due to their tunability, biocompatibility, and high transfection rate of siRNA.[29] We have developed a cationic micelles delivery system based on PEG-PLL-PLLeu hybrid polypeptides, which could be serve as a highly effective gene vectors,[30] and further demonstrated it was capable of co-delivering siRNA and docetaxel into cancer cell and achieving synergistic effect in vivo.[31]

Non-small cell lung cancer (NSCLC) accounts for over 85% of clinical lung cancer case.[32] It is reported that higher than 60% of NSCLC patients are diagnosed to have advanced or metastasis tumors, which is severly late for surgical resection.[33] Therefore, new treatment approaches are highly desired for NSCLC. In this study, we employed this polypeptide micelles for delivery of ZEB1 special siRNA to H460 NSCLC in vitro and vivo, we have showed that remarkable downregulation of the target gene, significant suppression of lung metastasis was triggered by siRNA-NPs. When co-delivering ZEB1 siRNA and DOX, a synergistic therapeutic effect was observed. These results indicated that suppressing ZEB1 expression and co-delivering

ZEB1 siRNA and DOX could provide a new therapeutic approach for NSCLC treatment.

Experimental

Materials

The Lipofectamine 2000 transfection kit (Invitrogen, Carlsbad, CA) was used according to the supplied protocol. Doxorubicin was purchased from Jinhe (China). Targeting human ZEB1 siRNA (sense:5'- UGCAUUUGCAGAUUGAGGCUGAUCA -3'and antisense: 5'- UGAUCAGCCUCAAUCUGCAAAUGCA-3'), negative control siRNA (NC-siRNA) and fluorescein-tagged siRNA (FAM-siRNA) were obtained from Shanghai GenePharma Co. Ltd. (Shanghai, China). Fluorescein-tagged siRNA (FAM-siRNA) was synthesized by modification of the 3'-end of the sense strand of the scrambled siRNA with fluorescein. Mouse primary antibodies against ZEB1, ABCG2, E-cadherin were purchased from abcam (UK). Rabbit primary antibody against SOX2 was purchased from Cell Signaling Technology (USA). GADPH and secondary antibodies conjugated with horseradish peroxidase (goat anti-mouse IgG HRP and goat anti-rabbit IgG HRP) were purchased from sigma (USA).

Preparation and Characterization of DOX Loaded Micelle NPs

The synthesis of the PEG-PLL-PLLeu (1:30:40) was carried out according to the ring-opening polymerization method as previously described.[29] Micelles were prepared by directly dissolving PEG-PLL-PLLeu copolymers in aqueous media with magnetic stirring for 2 h, followed by sonication for 30 min. DOX loaded micelle NPs (DOX-NP) was prepared as follows: PEG-PLL-PLLeu (10 mg) and DOX (2 mg) were dissolved in DMSO (6 ml) at room temperature under ultrasonic agitation, then the solution was added dropwise to pure water (6 ml) , and then moved to the dialysis bag with magnetic stirring for 24 h. The morphologies and zeta potentials of the self-assembled micelles were measured by transmission electronic microscopic (TEM) and Zetasizer Nano ZS (Malvern Instrument) at 25 °C. To determine DOX encapsulation efficiency (EE), DOX-loaded micelle solutions was diluted with DMSO in order to destroy the micellar structure and release the encapsulated DOX adequately. The concentration of DOX in the solution was quantified by Edinburgh F900 fluorescence spectroscopy using a previously established calibration curve.

Preparation of Complexed Micelle NPs and Gel Retardation Assay

siRNA, micelle NPs and DOX-NP were diluted with DEPC water at different concentrations. Desired amount of siRNA and NPs or DOX-NP were mixed and allowed to stand at room temperature for 30 mins before use. A series of complexes, such as siRNA-NP and siRNA-DOX-NP, were formed at different N/P ratios. The binding degree between siRNA and micelle NPs or DOX-NP was estimated using agarose gel electrophoresis. The electrophoretic mobility of micelleplex was visualized by a UV illuminator with SYBR Green I staining after electrophoresis on a 1.5% (w/v) agarose gel for 20 mins at 80 V in TAE buffer.

Cell Culture

The H460 cell line was obtained from American Type Collection (ATCC). H460 cells were maintained in RPMI-1640 medium supplemented with 10% fetal bovine serum (Gibco), 100 U/ml penicillin, and 100 μg/ml streptomycin at 37 °C with 5% CO_2.

Cellular Uptake Study

For the internalization experiment, H460 cells (4×10^4 cells/well) were seeded in 8-well glass bottom culture dish and incubated for 24 h before experiments. Cells were treated with different formulations at a concentration of 100 nM for FAM-labeled siRNA or 2 μg/ml DOX in serum-containing medium at 37 °C for 4 hours. After removal of the medium, cells were washed three times with the phosphate buffered saline (PBS) and fixed with 4% paraformaldehyde solution in PBS PH 7.4 at room temperature for 20 minutes. Then, the cells were counterstained with DAPI (4,6-diamidino-2-phenylindole) and imaged using confocal laser scanning microscopy. For endosomal escape stduy, the cells were treated and fixed as described above, then endosomes and nuclei were stained with Lysotracker Red and DAPI, respectively.

In vitro Cell Transfection

H460 cells (5×10^5) were seeded in 24-well culture plates overnight and allowed to grow until 60%~70% confluent. Various formulations were added to each well at a siRNA final concentration of 50 nM, followed by incubating the cells for 8 h, each well was replaced with fresh RPMI-1640 medium. Cells were harvested 48 h post-transfection for real-time PCR study, clony formation assay and matrigel invasion chamber assay. Alternatively, cells were harvested 72 h post-transfection for Western blot assay.

Real-time PCR Study

Total RNA from transfected cells was isolated using the AxyPrep Multisource total RNA Miniprep Kit (Axygen, USA) according to the protocol of manufacturer. Two micrograms of total RNA were transcribed into cDNA using the ReverTra Ace qPCR RT Kit (TOYOBO, Japan). Thereafter, 1 ul of cDNA was subjected to qRT-PCR analysis using the SYBR® Green Realtime PCR Master Mix (TOYOBO, Japan). Reactions were performed on a LightCycler480 real-time PCR system (Roche) and parameters consisted of Taq activation at 95 °C for 60 s, followed by 40 cycles of 95 °C for 30 s, 59 °C for 30 s and 72 °C for 30 s. Standard curves were generated and the relative amount of target gene mRNA was normalized to GAPDH mRNA. Specificity was verified by melt curve analysis. Primers used were shown in Table S1 (supplemental Information).

Western Blot Analysis

H460 cells were transfected with different formulations and further incubated for 72 h, and then resuspended in RIPA lysis buffer supplemented with complete protease inhibitor Cocktail (sigma, USA), The cell lysates were incubated on ice for 30 min and vortexed for 5 min, and then collected after centrifugation for 5min at 12,000 ×g. The protein concentration was determined using the BCA Protein Assay Kit (Thermo, Madison, WI). Cell lysates were separated on 12% acrylamide gels and transferred to nitrocellulose membranes (Millipore, Bedford, MA). Membranes were blocked for 1 hour in 5% skim milk and then incubated

overnight with monoclonal antibodies against ZEB1 (1:1000), ABCG2 (1:400) , SOX2 (1:1000), polyclonal antibodies against E-cadherin (1:2000) overnight. After incubation with anti-mouse or anti-rabbit IgG-HRP antibody for 1 hour, the relative content of the target proteins were detected by the ECL system (Pierce, USA).

Clony formation, Matrigel invasion chamber assay

H460 cells were treated with different formulations and further incubated for 48 h. Then cells were digested and suspensioned, the clonogenic potential of cells was determined by seeding approximately 300 cells/ well in 6-well plates. After 14 d of incubation, cells were stained with 0.1% crystal violet in PBS for 30min at room temperature. and colonies with > 50 cells were counted under dissection microscope. Invasion Chamber (BD BioCoat™ Matrigel™ Invasion Chamber) was used to study cell invasion of H460 cell post-transfection. After rehydrated matrigel inserts, the top chambers were seeded with RPMI-1640 (without growth factors) containing 4×10^4 cells, and the bottom chambers were filled with RPMI-1640 contained with various growth factors. After incubation for 22 h in a humidified tissue culture incubator, at 37 °C, 5% CO_2 atmosphere, the non-invading cells were removed from the upper surface of the membrane, the cells on the lower surface of the membrane were fixed with 100% methanol and stained with 0.1% crystal violet. The invaded cells were quantified by manual counting through the microscope.

Cell Proliferation and Cell Apoptosis Analysis

CCK-8 assay was utilized to evaluate the cytotoxicity of micelle NPs and different NP formulations. Cells (2×10^3 cells/well) were seeded into 96-well plates and incubated at 37 °C, 5% CO_2 overnight prior to treatment. Then the old medium was replaced with the medium containing the NPs over a wide range of concentrations (from 5 to 80 μg/mL NP) or Various NP formulations (containing 0.25 μg/mL DOX) and other controls. After 48 h (for NP) or 96 h (for different formulations) incubation, the medium was carefully removed and 100 ul medium supplemented with 10 ul CCK-8 solution were added. Followed by incubated for another 1 h, the absorbance at a wave-length of 450 nm of each well was measured by a microplate reader (Synergy 4, Bio Tec, USA). The cell viability (%) was calculated based upon the absorbance values relative to blank control. The experiment was repeated three times.

For cell apoptosis analysis, H460 cells cultured in 24-well plates were treated with the different formulations at a DOX dose of 0.25 μg/mL. After 96 h of treatment, the cells were harvested, and the Alexa Fluor 488 Annexin V/PI Cell Apoptosis Kit was used to detect and quantify apoptosis by BD Accuri C6 flow cytometer (USA).

Animals and Tumor Model

Female BALB/c nude mice (6-8 weeks old, weight around 20 g) were purchased from Shanghai Experimental Animal Centre of Chinese Academy of Sciences (Shanghai, China), and all animals received care in compliance with the guidelines suggestions for the Care and Use of Laboratory Animals. The procedures were approved by Shenzhen Institutes of Advanced Technology, Chinese Academy of Sciences Animal Care and Use Committee.

Antitumor activity was investigated in pulmonary metastatic H460 model and subcutaneous H460 model. To set up pulmonary metastatic H460 model, mice were injected intravenously with 100 μl of cell suspension containing 2×10^6 H460 cells. In subcutaneous H460 model, mice were injected subcutaneously with 100 ul of cell suspension containing 5×10^5 cells in the right flank. Tumor volume was determined by measuring tumor length (a) and tumor width (b) and calculated as $V = ab^2/2$.

Tumor Uptake and Tissue Distribution Study

To examine siRNA or DOX distribution in xenograft tumor，mice bearing subcutaneous tumors were i.v. injected with free FAM-labeled siRNA (1 mg/kg) or DOX (2 mg/kg) in different formulations: (1) Free FAM-siRNA, (2) FAM-siRNA-NP, (3) Free DOX, (4) DOX-NP (n=3 for each group). After 10 hours, the mice were sacrificed and the major organs including heart, liver, spleen, lung, kidney and tumor were collected. Images and FL semiquatitative biodistribution analysis of FAM-siRNA in those organs were detected using the ex/in vivo imaging system (CRi, Inc, USA). As DOX was not suitable for NIR FL imaging, tumor from DOX and DOX-NP groups were embedded in tissue-tek optimum cutting temperature compound (OCT) and frozen for cryosection. Tumor tissues were sectioned (10 μm thick) and imaged using a Leica TCS SP5 confocal microscope. For DOX systemic biodistribution study, the tissues were homogenized in lysis buffer and incubated at room temperature for 1h. The supernatant was collected after centrifugation at 12,000 ×g for 10 minutes. Then 100 μl supernatant was transferred to a 96-well plate and the fluorescence intensity of the sample was measured by a microplate reader (Synergy 4, Bio Tec, USA) at excitation wavelength of 485 nm and emission wavelength of 560 nm. DOX concentration in each sample was calculated from a standard curve.

***In vivo* gene knockdown study**

H460 subcutaneous tumor-bearing mice and H460 pulmonary metastasis-bearing mice were i.v. injected with siRNA in different formlations (n = 3 for each group, 0.4 mg siRNA/kg, one injection per day for 3 days). A day after the third injection, mice were killed and tumor samples were collected. Total RNA and total protein were isolated for quantitative real-time RT-PCR and Western blot analysis as described above.

***In vivo* tumor metastasis and growth inhibition study**

For tumor metastasis inhibition study, H460 metastasis-bearing mice were i.v. injected with siRNA in the nanoparticles on days 7 ,10 and 13. On day 50, the mice were killed, the tumor-bearing lungs were collected and tumor nodules in each lung were numbered. Then the lungs were fixed in 4% neutral buffered formalin, embedded in tissue-tek optimum cutting temperature compound (OCT), sectioned at 10 μm, stained with hematoxylin and eosin (H&E) and examined by a digital microscope. For tumor growth inhibition assay, when tumor size reached approximately 50~100 mm^3, subcutaneous tumor-bearing mice were randomly divided into six groups, and were i.v. injected various formulations, each of which is equivalent to a DOX dose of 0.8 mg/kg and siRNA dose of 0.4 mg/kg per injection. Body weights and tumor sizes were measured during the treatment

period.

Statistical analysis

All statistical analyses were performed by Student's t-test. Data were considered statistically significant when P value was <0.05.

Results and Discussion

Preparation and characterization of drug loaded micelle NPs

The polypeptide self-assembled a micelle structure in aqueous solution and exhibited the ability of simultaneous loading of siRNA and DOX. As shown in Figure 1A, DOX was encapsulated in the hydrophobic core, and siRNA was subsequently interacted with the PLL block to form the micelleplexes due to electrostatic interactions. The siRNA-DOX-NP complexes showed spherical morphology (Figure 1B), demonstrated by negative stain under the TEM image. The complexation of blank micelle NPs or DOX-NP with siRNA was investigated by agarose gel electrophoresis, respectively. As shown in Figure 1C, complete binding of siRNA occurred at a 3:1 molar ratio of nitrogen/phosphate (N/P ratio) in the micelle NPs and siRNA. The size and zeta potential of micelle NPs changed little after loaded DOX, the size of siRNA loaded DOX-NP increased from 115.5 ± 1.5 nm to 136.4±2.1 nm, and the zeta potential decreased from 55.26 ± 2.37 mV to 32.78 ± 1.82 mV(Figure 1D). The encapsulation efficiency (EE) of DOX was around 62.6% in our experiment, and DOX-NP were stable after storing for 1 month (the data was not shown). To estimate the safety of micelle NPs *in vitro*, H460 and 293T cells were treated with blank micelle NPs at different concentration, as shown in Figure 1E, the cell viabilities were higher than 81.2% and 83.3% respectively, even when the concentration of micelle NPs was up to 80 μg/mL, these results indicated that micelle NPs showed low cytotoxicity, which could be served as a safe carrier.

Uptake of siRNA and DOX *in vitro*

To investigate the delivery effciency of micelle NPs, we first analyzed the cellular uptake and intracellular distribution of siRNA. FAM-labeled oligo was used in order to visualize the cell uptake of siRNA. Lipofectamin 2000 was used as positive control. After 4 h of incubation, FAM-labeled oligo was evenly spread throughout the cytoplasm of H460 cells delivered by micelle NPs (Supplementary Figure S1A). On the contrary, FAM-labeled oligo showed punctate distribution delivered by Lipofectamin 2000. The results indacated the micelle NPs could effectively release its cargo to the cytoplasm. Then the simultaneous delivery of siRNA and DOX was demonstrated. As shown in Figure 1, a high degree of colocalization of the red (DOX) and green fluorescence (siRNA) distributed in the cytoplasm, which strongly demonstrating that siRNA and DOX were co-delivered into the H460 cells. We also use Lysotracker Red to stduy endosome escape efficiency, Figures 2B showed that siRNA in the siRNA-NP formation was able to escape from the endosome, as demonstrated by the separation of green (siRNA) and red (endosome) fluorescence in the cytoplasm.

Evaluation of ZEB1 knockdown efficiency

To estimate the gene silencing effect of the micelleplex in vitro, cellular mRNA was extracted and analyzed using real-time PCR and RT-PCR 48 h post transfection. Micelle NPs carrying 50 nM of target siRNA (siRNA-NP) and Lipofectamine 2000 carrying 50 nM of target siRNA (siRNA-Lipofectamin) led to approximately 72.9% and 76.7% knockdown of ZEB1 mRNA, respectively, whereas micelle NPs carrying Nonsense siRNA (NC-NP) showed no knockdown efficiency (Supplementary Figure S1B, S1C). We also examined ZEB1 protein expression by Western blot analysis 72 h post transfection, decreased ZEB1 protein expression was consistent with mRNA change (Supplementary Figure S1D). The result that siRNA-NP exhibited effective knockdown efficiency, which was similar to siRNA-Lipofectamin, indicating that siRNA delivered by micelle NPs could effectively suppress target gene expression in vitro, and polypeptide micelle NPs could be used as highly effective siRNA vectors.

ZEB1 knockdown reduced EMT and repressed CSC properties of H460 cells

To investigate the biological function and Therapeutic potential of knockdown ZEB1 in H460 cells, we detected the expression of E-cadherin, SOX2 and ABCG2 in mRNA and protein level. ZEB1 has been identified as an inducer of EMT, which is characterized by loss of epithelial markers like E-Cadherin.[34] Therefore, ZEB1 expression is often inversely correlated with E-cadherin expression. Moreover, ZEB1 is crucial for maintaining CSC properties, a negative feedback loop between ZEB1 and stemness-inhibiting microRNAs has been identified in some models such as pancreatic cancer.[13] SOX2 and ABCG2 are makers of CSC, and ABCG2 expression is also associated with resistance to a wide range of chemotherapeutic agents such as mitoxantrone, daunorubicin and doxorubicin.[35, 36] As is shown in Figure 3A, 3B, after knockdown of ZEB1, the mRNA expression of E-cadherin in H460 cells was significantly increased (3.15 fold increment), the mRNA expression of SOX2 and ABCG2 in H460 cells were dramaticlly decreased (64.6 % and 67.5 %, respectively), whereas the other controls did not cause this effect. mRNA expression alterations were subsequently accompanied by protein expression changes in a similar manner. Those results indicate that knockdown of ZEB1 could reduce EMT and the number of CSC expressing the markers in H460 cells.

ZEB1 silencing inhibited H460 cells invasion and sensitized the cells to DOX

EMT not only enable the detachment of cells from each other and increases cell mobility, but also confer on cells defining features of CSC, such as increased drug resistance and resistant to apoptosis. therefore, it is possible that micelle NPs mediated knockdown of ZEB1 could inhibit H460 cells metastasis and sensitize the cells to chemotherapy drug. Colony formation assay was used to test the effect of ZEB1 siRNA-NP, the results showed that siRNA-NP significantly inhibited colony formation of H460 cells compared to untreated control and NC-NP group (Figure 4A). For cancer cells to invade surrounding tissue, the cells must degrade the underlying basement membrane. Transwell assay were conducted to evaluate the activity of H460 to invade the extracellular matrix. As shown in Figure 4B, a

stronger inhibitory effect on invasion properties of H460 cells was observed in siRNA-NP group, indicating suppression of ZEB1 expression by siRNA-NP reduced the metastatic potential of H460 cells.

We further tested the therapeutic effect of simultaneous delivery of ZEB1 siRNA with DOX at a low concentration (0.25 μg/mL), as shown in Figure 5A, Cell proliferation was determined by CCK-8 assay, siRNA-NP and DOX-NP inhibited cell proliferation to 85.1% and 52.3%, respectively. In comparison, siRNA-DOX-NP and DOX-NP combining with siRNA-NP both significantly reduced cell viability to approximately 20%, achieving a synergistic inhibitory effect. Cell apoptosis was also evaluated after treating H460 cells with different formulations, siRNA-NP and DOX-NP were able to induce cell apoptosis (including the early apoptotic cells and fully apoptotic cells) to 9.6% and 9.8%, respectively, but not surprisingly, simultaneous delivery of ZEB1 siRNA with DOX induced cell apoptosis to 36.5%, with a synergistic effect as well (Figure 5B, 5C), which was similar to cell proliferation assay described above. Collectively, these results suggested that ZEB1 knockdown sensitized H460 cells to DOX treatment and ZEB1 siRNA in combination with DOX could be a potential therapy strategy for NSCLC.

Uptake and biodistribution of siRNA and DOX *in vivo*

Organ distribution of FAM-labeled siRNA delivered by micelle NPs or delivered as free siRNA without any transfection reagent in tumor-bearing mice was examined using small animal imaging technology. As shown in Figure 6A, 6B, after i.v. injection of 10 h, free siRNA group showed most of siRNA accumulated in the liver, follow by kidney and lung. In contrast, siRNA-NP formulation dramatically increased the accumulation of siRNA in the tumor. It should be noted that the FL signals and intensity of siRNA in liver and kidney from siRNA-NP group are much weaker than free siRNA group. Although a moderate fluorescence signal was present in the tumor from free siRNA group, it is worth noting that free siRNA cannot easily enter cytoplasm and achieve its functions.

We studied DOX uptake of H460 tumor tissue in the tumor-bearing mice after i.v. injections of 10 h using confocal microscopy. As shown in Figure 6C, DOX-NP showed stronger cytosolic delivery of DOX in the tumor tissue than free DOX, of which the fluorescence signal of DOX was hardly detectable in tumor tissues. The distribution of DOX in the tumor was heterogeneous. In the quantitative analysis (Figure 6D), liver, kidney, and spleen showed stronger uptake of free DOX than DOX-NP formulation. whereas DOX-NP showed stronger DOX delivery in the tumor tissue than free DOX.

Taken together, those results demonstrated that the micelle NPs efficiently delivered siRNA and DOX to the tumor tissue, as well as reduced its accumulation in liver and kidney, which could be explained the long circulation and enhanced permeability and retention effect (EPR) of the PEG-PLL-PLLeu micelle delivery system.

ZEB1 knockdown reduced EMT and repressed CSC properties of H460 xenograft tumours

Encouraged in the excellent EPR effect of the micelle NPs, we further verified whether the biological function of ZEB1 siRNA could also be achieved in vivo. The subcutaneous tumor-bearing mice and lung metastases–bearing mice were treated with different formulations with three consecutive i.v. administrations. Tumor mass was excised 24 h after the last injection, mRNA and protein expression were analyzed. As shown in Figure 7, xenografts from mice treated by the micelle NPs containing ZEB1 siRNA showed reduced ZEB1 mRNA levels (37% of the PBS control in subcutaneous tumors, 45% of the PBS control in lung metastases tumors). Meanwhile, upregulated E-cadherin mRNA levels and downregulated SOX2 and ABCG2 mRNA levels were observed in tumor sites after ZEB1 knowndown, which were supported by Western blot analyses (Figure 7E). These results demonstrated that systemic delivery of ZEB1 siRNA could effciently knockdown the target gene expression, as well as reduced EMT and repressed CSC properties of H460 cells in xenograft tumours.

Tumor metastasis inhibition by micelle NPs containing siRNA

Pulmonary metastatic H460 model was used to elucidate the tumor metastasis inhibition effect of siRNA-NP, the lung metastasis–bearing mice were i.v. injected with different formulations on days 7, 10 and 13 (siRNA dose 0.4 mg/kg). As shown in Figure 8A, 8B, three injections of siRNA-NP dramatically decreased the number of tumor nodules in lung, whereas mice treated with NC-NP had no therapeutic effect. Histological analysis of the tumor by hematoxylin and eosin (H&E) staining showed that the growth of the tumor nodules in the lung was significantly inhibited by siRNA-NP. The results demonstrated that ZEB1 siRNA delivered by the micelle NPs could significantly suppress tumor metastasis.

Tumor growth inhibition by micelle NPs containing siRNA and DOX

Subcutaneous H460 model was used to investigate the therapeutic effect of the codelivery of siRNA and DOX. Mice were i.v. injected with DOX-siRNA-NP or various other formulations every three days for five times. According to the Figure 9A, NC-NP hardly affected tumor growth comparing with PBS treatment, DOX-NP at a low dose (DOX 0.8 mg/kg per injection) showed little anti-tumor effect, while siRNA-NP (siRNA 0.4 mg/kg per injection) showed moderate inhibition of tumor growth. However, simultaneous delivery of the same doses of DOX and siRNA by siRNA-DOX-NP and DOX-NP+ siRNA-NP exhibited dramatical inhibition of tumor growth. In addition, the mice from different groups did not show obvious weight loss compared to the PBS control, indicating that the micelle NPs were safety nanocarriers (Figure 9C). Survival of tumor bearing mice was also monitored following therapy. The survival in siRNA-NP group was significantly longer compared with NC-NP, DOX-NP and PBS groups, and simultaneous delivery of DOX and siRNA resulted in a more prolonged survival (Figure 9B). These results suggested that the combination of siRNA and DOX co-delivered by micelle NPs could synergistically inhibit tumor growth and enhanced the therapeutic effect.

Conclusions

In this study, We demonstrated the use of a multifunctional

nanocarrier to overcome metastasis and drug resistance by delivering ZEB1siRNA or codelivering ZEB1siRNA and DOX. The micelleplex system showed excellent passive targeting effect and reduced hepatotoxicity and nephrotoxicity. siRNA-NP could efficiently downregulated the expression of target gene ZEB1 and significantly reduce the metastasis in the lung. Through co-delivery of DOX and ZEB1 siRNA in the siRNA-DOX-NP formulation sensitized H460 cells to DOX chemotherapy, cell apoptosis was enhanced and resulted in synergistic therapeutic effect in vivo. To our knowledge, this is the first study of systemic delivery of ZEB1 siRNA for cancer therapy, which could also help us understand the function and mechanism of ZEB1 in NSCLC development, the therapeutic effects of knockdown ZEB1 were associated with reducing EMT and repressing CSC properties. Therefore, ZEB1 siRNA in combination with DOX co-delivery by this polypeptide micelles provides a promising approach for cancer therapy.

Acknowledgements

The authors gratefully acknowledge support for the National Natural Science Foundation of China (Grant No. 81071249, 81171446 and 20905050), Guangdong Innovation Team of Low-cost Healthcare, Science and Technology Key Project of Guangdong (2009A030301010) and Shenzhen(CXB201005250029A, JC201005270326A, JC201104220242A, JC201005260247A). (CXB201005250029A, JC201005270326A, JC201104220242A, JC201005260247A).

Notes and references

Guangdong Key Laboratory of Nanomedicine, Shenzhen Key Laboratory of Cancer Nanotechnology, Institute of Biomedicine and Biotechnology, Shenzhen Institutes of Advanced Technology, Chinese Academy of Sciences, Shenzhen 518055, Guangdong (P. R. China). Fax: +86 755 86392299; Tel: +86 755 86392210; E-mail: lt.cai@siat.ac.cn

1 A. Singh and J. Settleman, *Oncogene*, 2010, **29**, 4741-4751.
2 Z. Wang, Y. Li, A. Ahmad, A. S. Azmi, D. Kong, S. Banerjee and F. H. Sarkar, *Drug resistance updates*, 2010, **13**, 109-118.
3 A. Voulgari and A. Pintzas, *Biochimica et biophysica acta*, 2009, **1796**, 75-90.
4 T. Arumugam, V. Ramachandran, K. F. Fournier, H. Wang, L. Marquis, J. L. Abbruzzese, G. E. Gallick, C. D. Logsdon, D. J. McConkey and W. Choi, *Cancer research*, 2009, **69**, 5820-5828.
5 R. Xiang, D. Liao, T. Cheng, H. Zhou, Q. Shi, T. S. Chuang, D. Markowitz, R. A. Reisfeld and Y. Luo, *British journal of cancer*, 2011, **104**, 1410-1417.
6 M. Konopleva, Y. Tabe, Z. Zeng and M. Andreeff, *Drug resistance updates*, 2009, **12**, 103-113.
7 S. A. Mani, W. Guo, M. J. Liao, E. N. Eaton, A. Ayyanan, A. Y. Zhou, M. Brooks, F. Reinhard, C. C. Zhang, M. Shipitsin, L. L. Campbell, K. Polyak, C. Brisken, J. Yang and R. A. Weinberg, *Cell*, 2008, **133**, 704-715.
8 K. Polyak and R. A. Weinberg, *Nature reviews. Cancer*, 2009, **9**, 265-273.
9 A. S. Adhikari, N. Agarwal, B. M. Wood, C. Porretta, B. Ruiz, R. R. Pochampally and T. Iwakuma, *Cancer research*, 2010, **70**, 4602-4612.
10 Y. P. Liu, C. J. Yang, M. S. Huang, C. T. Yeh, A. T. Wu, Y. C. Lee, T. C. Lai, C. H. Lee, Y. W. Hsiao, J. Lu, C. N. Shen, P. J. Lu and M. Hsiao, *Cancer research*, 2013, **73**, 406-416.
11 A. Bandyopadhyay, L. Wang, J. Agyin, Y. Tang, S. Lin, I-T.Yeh, K. De and L. Sun, *PLoS One*. 2010, **5**, e10365.
12 S. Spaderna, O. Schmalhofer, M. Wahlbuhl, A. Dimmler, K. Bauer, A. Sultan, F. Hlubek, A. Jung, D. Strand, A. Eger, T. Kirchner, J. Behrens and T. Brabletz, *Cancer research*, 2008, **68**, 537-544.
13 U. Wellner, J. Schubert, U. C. Burk, O. Schmalhofer, F. Zhu, A. Sonntag, B. Waldvogel, C. Vannier, D. Darling, A. zur Hausen, V. G. Brunton, J. Morton, O. Sansom, J. Schuler, M. P. Stemmler, C. Herzberger, U. Hopt, T. Keck, S. Brabletz and T. Brabletz, *Nature cell biology*, 2009, **11**, 1487-1495.
14 C. L. Chaffer, N. D. Marjanovic, T. Lee, G. Bell, C. G. Kleer, F. Reinhardt, A. C. D'Alessio, R. A. Young and R. A. Weinberg, *Cell*, 2013, **154**, 61-74.
15 Y. Takeyama, M. Sato, M. Horio, T. Hase, K. Yoshida, T. Yokoyama, H. Nakashima, N. Hashimoto, Y. Sekido, A. F. Gazdar, J. D. Minna, M. Kondo and Y. Hasegawa, *Cancer letters*, 2010, **296**, 216-224.
16 Y. Liu, X. Yan, N. Liu, J. Zhou, J. Liu, H. Pang, J. Cao, Y. Liu, Y. Wang, L. Liu and H. Zhang, *Journal of cancer research and clinical oncology*, 2012, **138**, 1329-1338.
17 M. Horio, M. Sato, Y. Takeyama, M. Elshazley, R. Yamashita, T. Hase, K. Yoshida, N. Usami, K. Yokoi, Y. Sekido, M. Kondo, S. Toyokuni, A. F. Gazdar, J. D. Minna and Y. Hasegawa, *Annals of surgical oncology*, 2012, **19**, S634-645.
18 M. E. Davis, J. E. Zuckerman, C. H. Choi, D. Seligson, A. Tolcher, C. A. Alabi, Y. Yen, J. D. Heidel and A. Ribas, *Nature*, 2010, **464**, 1067-1070.
19 Y. Chen, X. Zhu, X. Zhang, B. Liu and L. Huang, *Molecular therapy,* 2010, **18**, 1650-1656.
20 H. Yu, Y. Zou, L. Jiang, Q. Yin, X. He, L. Chen, Z. Zhang, W. Gu and Y. Li, *Biomaterials*, 2013, **34**, 2738-2747.
21 J. Li, Y. Yang and L. Huang, *Journal of controlled release : official journal of the Controlled Release Society*, 2012, **158**, 108-114.
22 P Sengupta, S Basu, S Soni, A Pandey, B Roy, M. S. Oh, K. T. Chinc, A. S. Paraskar, S. Sarangi and Y. Connor, Proc. Natl. Acad. Sci. U. S. A. 2012, 109, 11294-11299.
23 X-H. Peng, Y. Wang, D. Huang, Y. Wang, H. J. Shin, Z. Chen, M. B. Spewak, H. Mao, X. Wang and Y. Wang, *ACS Nano*. 2011, **5**, 9480-9493.
24 W. C. Zamboni, *The oncologist*, 2008, **13**, 248-260.
25 H. Meng, W. X. Mai, H. Zhang, M. Xue, T. Xia, S. Lin, X. Wang, Y. Zhao, Z. Ji and J. I. Zink, *ACS Nano*, 2013, **7**, 994-1005.
26 D. Cheng, N. Cao, J. Chen, X. Yu and X. Shuai, *Biomaterials*, 2012, **33**, 1170-1179.
27 Y. Chen, J. J. Wu and L. Huang, Molecular therapy, 2010, 18, 828-834.
28 C. He, K, K. Lu, D. Liu and W. Lin, Journal of the American Chemical Society, 2014, 136, 5181−518418.
29 M. Creixell and N. A. Peppas, *Nano Today*, 2012, **7**, 367-379.
30 J. Deng, N. Gao, Y. Wang, H. Yi, S. Fang, Y. Ma and L. Cai, *Biomacromolecules*, 2012, **13**, 3795-3804.
31 C. Zheng, M. Zheng, P. Gong, J. Deng, H. Yi, P. Zhang, Y. Zhang, P. Liu, Y. Ma and L. Cai, *Biomaterials*, 2013, **34**, 3431-3438.
32 A. Jemal, M. J. Thun, L. A. Ries, H. L. Howe, H. K. Weir, M. M. Center, E. Ward, X. C. Wu, C. Eheman, R. Anderson, U. A. Ajani, B. Kohler and B. K. Edwards, *Journal of the National Cancer Institute*, 2008, **100**, 1672-1694.
33 W. Pao and J. Chmielecki, *Nature reviews. Cancer*, 2010, **10**, 760-774.
34 M. A. Huber, N. Kraut and H. Beug, *Current opinion in cell biology*, 2005, **17**, 548-558.
35 L. Doyle and D. D. Ross, *Oncogene*, 2003, **22**, 7340-7358.
36 Y. Folmer, M. Schneider, H. E. Blum and P. Hafkemeyer, *Cancer gene therapy*, 2007, **14**, 875-884.

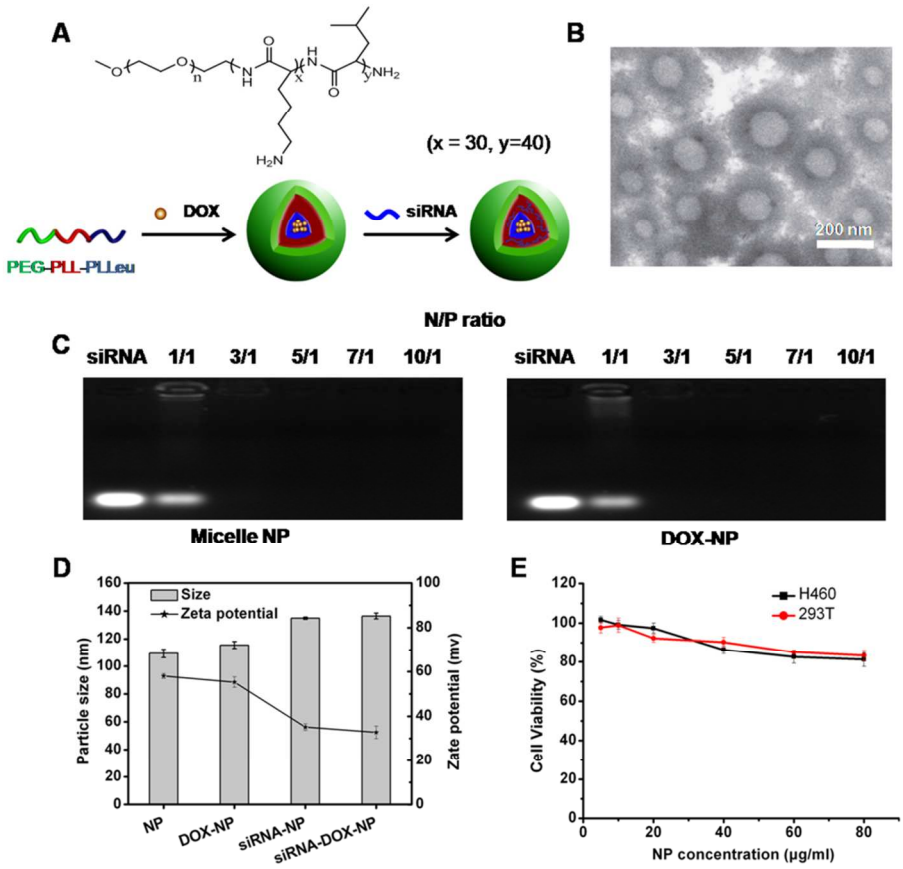

Figure 1. Preparation and characterization of drug loaded micelle NPs. (A) Schematic diagram of self-assembled cationic micelle and loading of siRNA and DOX. (B) Transmission electronic microscopic image of siRNA-DOX-NP complexes. (C) Binding ability of Blank NP and DOX-NP to siRNA at different ratios of nitrogen in carrier to phosphate in siRNA (N/P ratio) demonstrated by the agarose gel retardation assay. (D) Size and zeta potential change after nano-complexes formation. (E) Cytotoxicity evaluation of micelle NP on H460 and 293T cells . Data are mean ± SE (n=5).

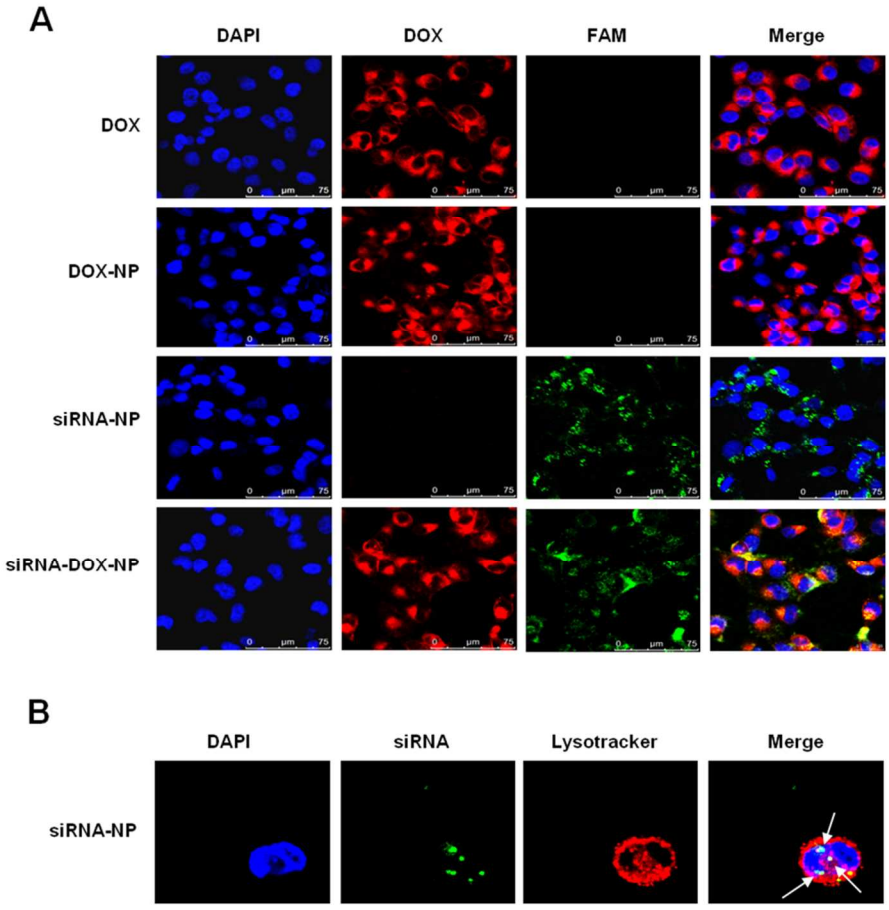

Figure 2. Uptake of siRNA and DOX in vitro. Confocal laser scanning microscope (CLSM) image of intracellular distribution of DOX and siRNA in H460 cells after incubation with DOX, DOX-NP, siRNA-NP and siRNA-DOX-NP for 4h. Fluorescence signal of DOX was observed in red. The siRNA was labeled with FAM (green). The nucleus was counterstained with DAPI (blue). (B) siRNA successfully escaped from endosomes in H460 cells was proved by the separation of red and green fluorescence (white arrows). Endosomes were stained with Lysotracker Red.

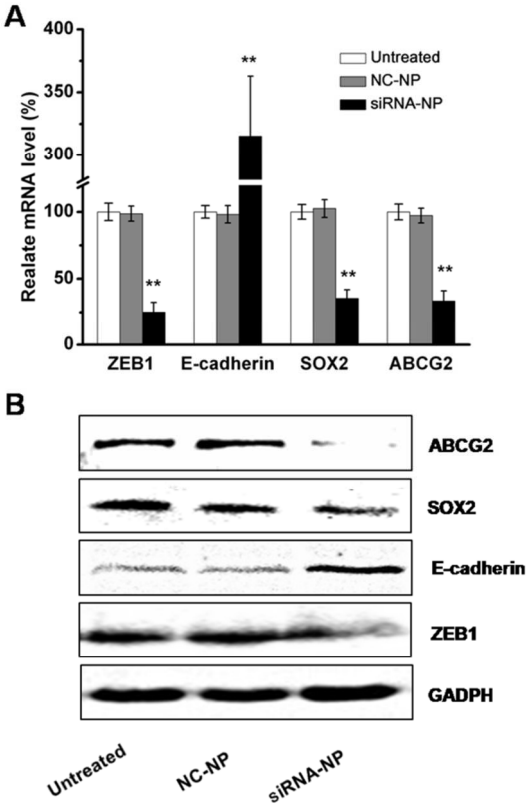

Figure 3. ZEB1 knockdown reduce EMT and repress cancer stem cell properties in H460 cells. (A) Relative mRNA level of ZEB1, E-cadherin, SOX2 and ABCG2 after transfection of H460 cells with different formations quantified by real-time PCR analysis. Incubation time: 48 h. (B) Western blot analysis of ZEB1, E-cadherin, SOX2 and ABCG2 protein expression after treatment of H460 cells with different formulations. The concentrations of ZEB1 siRNA and NC siRNA were 50 nM. Incubation time: 72 h. $^{**}p < 0.001$ as compared with controls. Data are mean ± SD (n = 3).

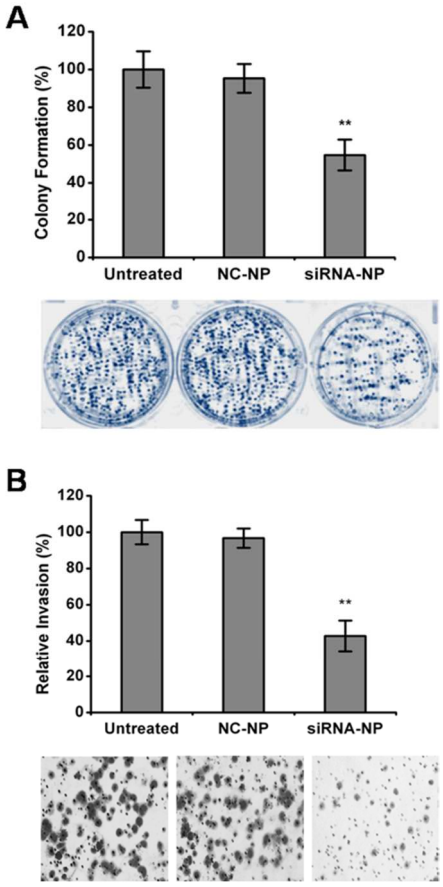

Figure 4. In vitro cellular evaluation of ZEB1 siRNA-NP. (A) Liquid colony formation assay of H460 cells after transfected with different formulations (n = 3). (B) Matrigel invasion chamber assay of H460 cells, Histogram showing the quantification of H460 cells invasion effciency. H460 cells transfected with ZEB1 siRNA or nonsense siRNA were plated on matrigel-coated filters and the invasive cells were fixed, stained with crystal violet, and counted (n = 3). $^{**}p < 0.001$ as compared with controls.

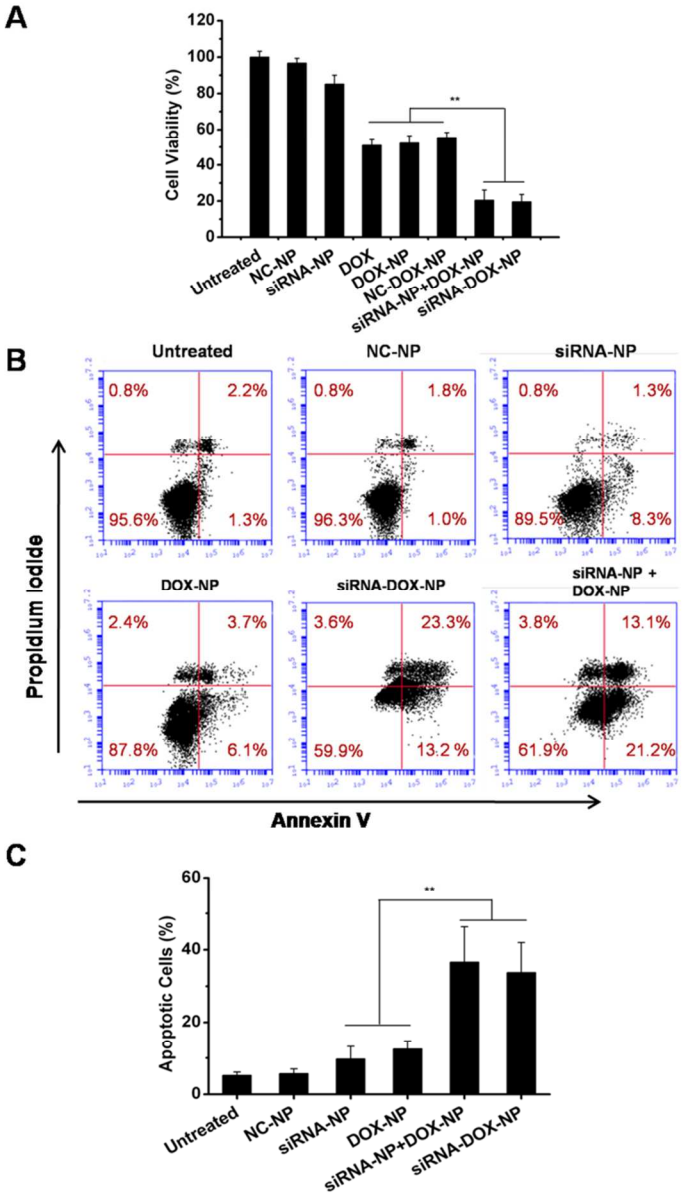

Figure 5. In vitro ZEB1 knockdown induces H460 cells sensitivity to DOX treatment. (A) Effect of co-delivery of ZEB1 siRNA and DOX by micelleplex on the proliferation of H460 cells (CCK-8 assay, n = 5). DOX concentration: 0.25 μg/mL; siRNA concentration: 50 nM. (B)Flow cytometer analysis of the apoptosis and necrosis cells after incubation with different formulations. The early apoptotic cells are presented in the lower right quadrant (V-FITC+/PI-), and late apoptotic cells are presented in the upper right quadrant (V-FITC+/PI+). (C) Proportion of apoptotic cells after different treatment (n = 3) . $^{**}p < 0.001$. Data are mean ± SD.

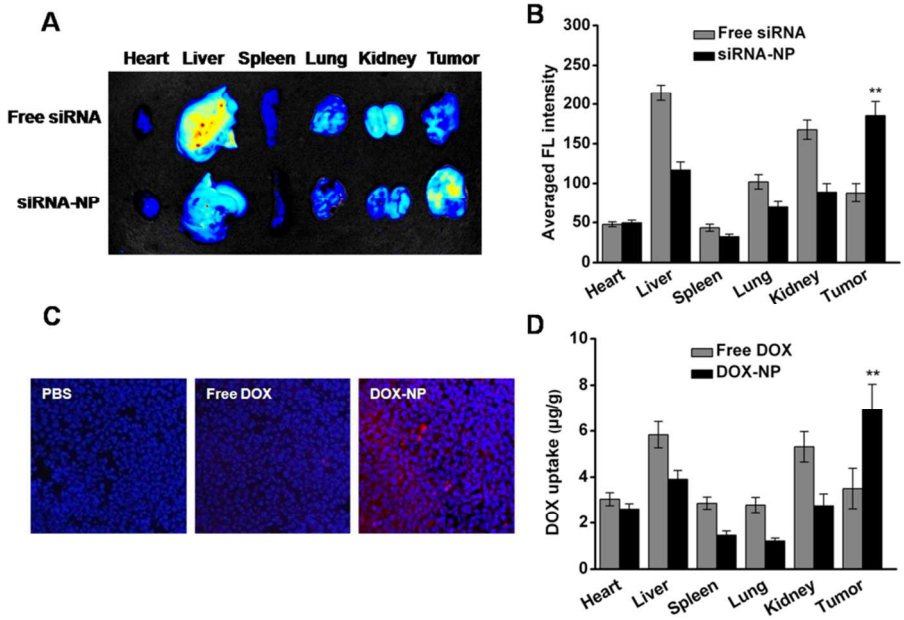

Figure 6. Delivery of siRNA and DOX in vivo. (A) Localization of labeled siRNA in tumor-bearing mice by a biophotonic-imaging based analysis after i.v. injectiontion of free siRNA and siRNA-NPs of 10h. The intensity of the fluorescence signal was analyzed in isolated hearts, livers, spleens, lungs, kidneys and tumors from the mice. (B) Semiquantitative biodistribution of siRNA in nudemice determined by the averaged FL intensity of organs and tumors. n = 3.**$P < 0.01$ compared with free siRNA group. (C) Fluorescence signal of DOX in H460 tumor tissue observed by confocal microscopy. (D) Tissue distribution of DOX in different formulations. n = 3. **$P < 0.01$ compared with free DOX group.

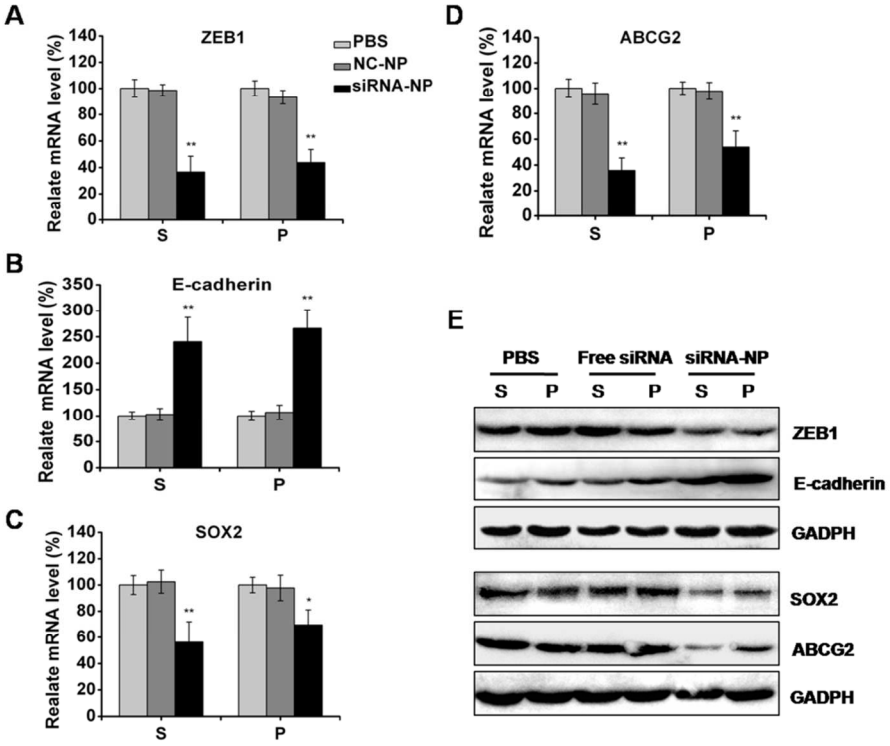

Figure 7. ZEB1 knockdown reduce EMT and repress cancer stem cell properties in subcutaneous tumor model and pulmonary metastatic tumor model. (S: subcutaneous tumor; P: pulmonary metastatic tumor) (A) ZEB1 (B) E-cadherin (C) SOX2 (D) ABCG2 mRNA expressions after different treatments. (F)) Western blot analysis of ZEB1, E-cadherin, SOX2 and ABCG2 after i.v. injections of different formations. *$P < 0.05$, **$P < 0.01$ compared with PBS controls.

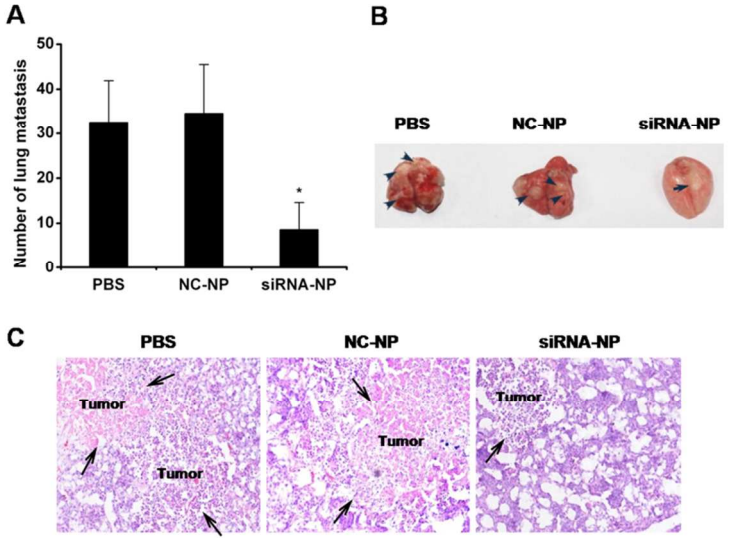

Figure 8. Tumor metastasis inhibition by ZEB1 siRNA-NP in vivo. (A) siRNA-NP inhibited metastasis in pulmonary metastatic H460 model. H460 metastasis-bearing mice were i.v. injected with siRNA in the nanoparticles on days 7 ,10 and 13, and tumor nodules in each lung were numbered on day 50 (n = 5). (B) Representative photographs of tumor-bearing lungs in each treatment group. (C) Histological staining of the tumor-bearing lungs after treatment (arrow: tumor nodules). *$P < 0.05$ compared with PBS controls.

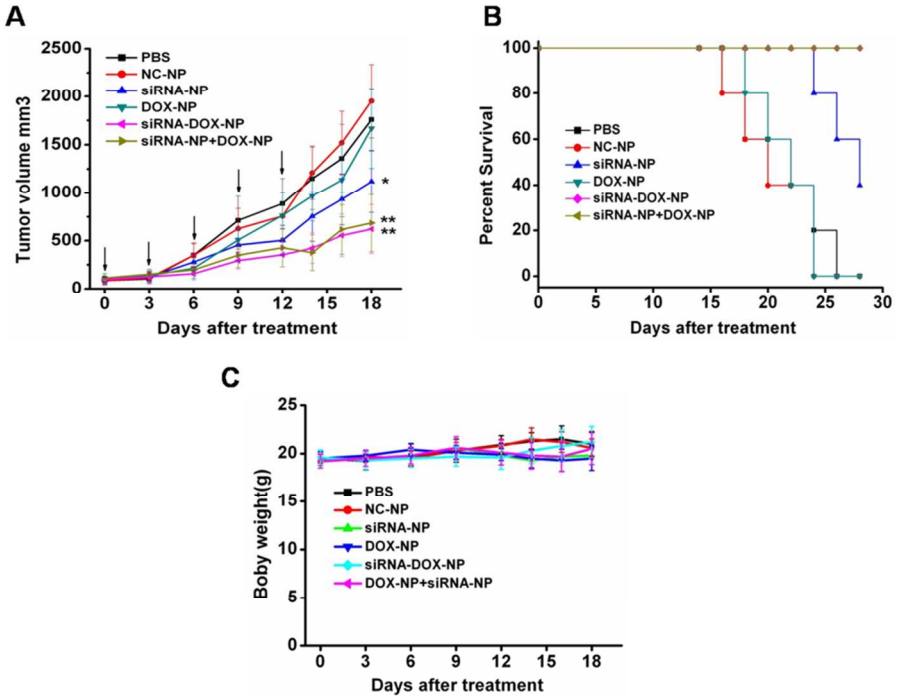

Figure 9. Tumor growth inhibition in vivo. (D) Inhibition of subcutaneous H460 tumor growth by DOX-siRNA-NP in comparison with various formulations (n = 5). (E) The body weights and (F) Survival rates of the mice bearing subcutaneous tumors in all groups. H460 subcutaneous tumor-bearing mice received one i.v. injection every other day for five times. (Dose per injection: DOX 0.8 mg/kg and siRNA 0.4 mg/kg, n=5). *$p < 0.05$, **$p < 0.001$ compared with PBS controls.